J Math Chem (2009) 45:330–353
DOI 10.1007/s10910-008-9409-0

ORIGINAL PAPER

Aromaticity of corazulenic fullerenes

Mircea V. Diudea · Aniela E. Vizitiu

Published online: 7 August 2008

Abstract A novel class of non-classical fullerenes, having pentagon–heptagon pairs, as in azulene, is modeled. The various coverings, sometimes alternating azulenic and benzenic units, are designed by some new sequences of map operations or generalized operations. The hypothetical azulenic fullerenes are characterized by PM3 semiempirical data and POAV1 strain energy SE. Their aromaticity is discussed in the light of several criteria. The HOMA index of aromaticity enabled evaluation of global and local aromaticity of the designed fullerenes.

Keywords Fullerenes · Azulenic fullerenes · Tessellation · Map operations · Aromaticity · Local aromaticity

1 Introduction

The aromatic character is a multi-conditional molecular property, including energetics, electronic structure, magnetic response, geometric characteristics or chemical behaviour [1–3]. Consequently, various orderings are expected in sets of molecules with respect to different aromaticity criteria. The above criteria have been detailed in a recent review by Randić [3] and we limit here to point out some particular aspects encountered in the newly proposed azulenic fullerenes.

The *structural/geometric criterion* of aromaticity is the most important criterion to be used in the hereafter discussion, thus we will focus on structural-geometric aspects useful in defining the aromaticity in the newly proposed cages.

The well-known theory of benzenoid faces to give the most aromatic character is due to Clar. This theory has attracted attention of many theorists [2–9].

M. V. Diudea (✉) · A. E. Vizitiu
Faculty of Chemistry and Chemical Engineering, Babes-Bolyai University, 400028 Cluj, Romania
e-mail: diudea@gmail.com

A Clar structure [10,11] is a valence structure having the maximal number of disjoint aromatic π-sextets. It can be drawn by superposing all the Kekulé structures with the highest degree of freedom [3]. Aromatic π-sextets are defined as six π-electrons localized to a single benzene ring separated from adjacent rings by formal CC single bonds.

A polyhedral map may have a perfect Clar PC structure, which is a set of disjoint faces (built up on all vertices in M) whose boundaries form a 2-factor. Recall that a k-factor is a regular k-valent spanning subgraph. A PC structure is associated with a Fries structure, [12] which is a Kekulé structure having the maximum possible $(v/3)$ number of benzenoid (alternating single-double edge) faces. A Kekulé structure is a set of pairwise disjoint edges/bonds of the molecule (defined over all its atoms) that coincides with a perfect matching and a 1-factor in Graph Theory [13]. A trivalent polyhedral graph, like that of fullerenes, has a PC structure if and only if it has a Fries structure [14].

Note that, only in polyhex structures (e.g., polyhex tori, where the assignment empty/full can be interchanged between two adjacent hexagons), the PC structure consists of $v/3$ disjoint hexagons (i.e., a 2-factor), as previously Clar suggested. In fullerenes, the PC structure must include all the odd faces (e.g., pentagons), usually assigned as empty π-electron faces. However, the associate Fries structure ensures the full resonance (i.e., conjugation, double-simple bond alternation) [14].

Such structures represent *totally resonant sextet* TRS benzenoid molecules which it is expected to be extremely stable, according to the VB theory [14–16]. Fully benzenoid hydrocarbons are $6n$ π-electron systems, whose Clar structures have only disjoint benzene rings, mutually connected by CC single bonds [3]. The concept of *total/fully-resonant* coverings (mainly benzenoids) has been discussed by several authors [16–25].

Leapfrog [26,27] *Le* is the only map operation providing PC transforms (Fig. 1).

Patterns larger than benzene, e.g., naphthalene or azulene (i.e., a pair of pentagonal-heptagonal carbon rings) have been considered with respect to the Clar theory [10,11]. By extension, Diudea [28–31] has proposed corannulenic supra-faces (eventually called *flowers*).

A coronene-like flower, i.e., an [n]annulene, or [n]circulene, is symbolized as [n:x, y]Fw, with n, x, y being the folding of the core and its surrounding polygonal faces, respectively. Such flowers could appear either as intersect, joint or disjoint units. Joint corannulenic flowers [n:x, y]JFw are provided by Capra *Ca* map

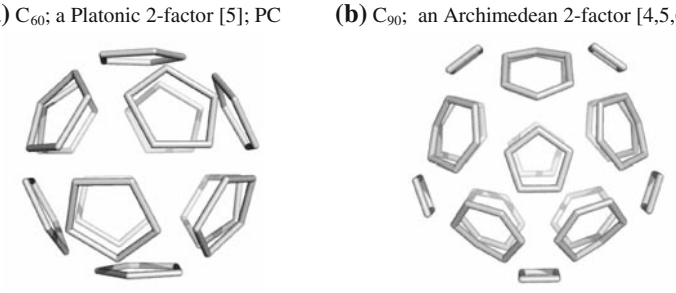

Fig. 1 Perfect Clar PC structures embedded in the sphere

operation while disjoint corannulenic flowers [n:x, y]DFw by some sequences of operations (e.g., $Le\&Q$; $Q_{(4,0)c}\&Tr_s$) or by the generalized $Le_{2,2}$ operation. Examples of corannulenic covering have been described elsewhere [29,30]. Note that PC and corannulenic DFw and JFw coverings account for the maximum possible ($v/3$) number of benzenoid faces, being an important structural feature defining the aromatic character.

A tiling is called Platonic if it consists of a single type of faces (similar to the Platonic solids). Archimedean is that tiling consisting of more than one (usually two) type(s) of faces. Platonic and Archimedean will refer here to only flowers' tessellation. Recall the five Platonic polyhedra and their symbols herein used: T (tetrahedron), O (octahedron), C (cube), D (dodecahedron, and I (icosahedron). The dual pairs are: $T\&T$ (self-dual); $O\&C$ and $D\&I$.

Our CageVersatile program [32] enables the flower embedding in surfaces of any genera and lattices of any vertex degree.

The supra-organized corannulenic units are expected to contribute to the stability of the whole molecule [28,33,34]. Semiempirical calculations (with the PM3 Hamiltonian) proved in part this expectation [30].

Note that coronene itself [6:6_6]Fw is not a totally resonant hydrocarbon [3] because any one Kekulé structure leaves some carbon atoms outside sextet rings. However, Clar proposed [35] that if the three sextets of coronene can migrate into the neighboring rings, an extra ring current will be formed. Thus, the sextet migration current is an argument in favor of the coronene enhanced aromaticity (compared to some other polycyclic hydrocarbons, e.g., naphthalene and anthracene) [36].

According to the magnetic criterion, the π-electron delocalization is required, with direct consequences on the magnetic properties, as reflected in the diamagnetic susceptibility and NMR chemical shifts. These effects can be rationalized in terms of ring currents induced by the external field. Ring-current effects have long been recognized as important indicators for aromaticity [3]. Depending on the number of π-electrons, diatropic or paratropic ring currents may occur.

Counter circulation of "rim and hub" currents is a characteristic of the corannulenes [n]Fw, as shown by the ipsocentric [37] CTOCD (continuous transformation of origin of current density) calculations [38,39]. This is one reason for the need of a disjoint DFw structure.

Based to the geometric criterion, an index of aromaticity, called HOMA (harmonic oscillator model of aromaticity) [40–45] was derived on the difference between the actual CC and the CC equalized bond lengths. The data in the following tables are calculated, cf. [45]. Within a single polycyclic conjugated structure, different rings normally show different local aromaticity [46] which can be accounted for by the HOMA values (ranging from 1 for benzene to about 0 for non-aromatic and negative values for anti-aromatic molecules).

Clearly, the aromaticity is a multi-dimensional phenomenon [47,48]. Even so, the structural features of molecules have to prevail, in the aromaticity assessment, over the observable properties, as Kekulé himself has stressed in the early days of this theory [3].

However, fullerenes are far from the "super-aromatic" dream of researchers, they approaching rather a "super-alkenic" character [49] with the additions the most favored

reactions. The electron deficiency of these molecules arises from the presence of 12 pentagons, instead of hexagons, in the sheet of graphite, needed to close a cage.

The paper is organized as follows. Section 2 presents the main annulenic flowers encountered in the new cades herein proposed, with their energetics, π-electron distribution and aromaticity in terms of HOMA index. Sections 3 and 4 present in detail several map operation sequences and their flower patterns and coverings, starting from Platonic solids and small regular cages, respectively. Section 5 deals with the retro Endo–Kroto reaction, possibly occurring in fullerenes. The article ends with conclusions and references.

2 Annulenic flowers

Annulenic/circulenic flowers, [28] generalizing the corannulenic flowers $[n{:}6_n]$Fws, can be achieved via map operation sequences. Any sequence of operations can be applied to any cage but we look here for minimal size faces, eventually of interest for chemists. By this reason, (triangulated) Platonics or other small cages (i.e., fullerenes) are used as starting cages.

We focused attention on corazulenic flowers, as the main Fw patterns in a covering, but others, like coronene, sumanene, etc., which often appear as intersected/superposed "counterpart" co-Fws, were also studied. Of course, the attribute Fw and co-Fw are interchangeable. The covering by a sequence of operations is given in terms of supra-faces.

When the operation sequence is commutative, the dual-pair will produce either non-distinguishable transforms or different transforms leading to a unique Stone-Wales [50] SW edge-rotated product. The SW isomerization was mainly performed on corazulenic supra-faces ($[n{:}(7(5c))_n]$Fw or $[n{:}(7(5d))_n]$Fw), taken here as the main Fw patterns, and used for naming these fullerenes. The name will include the actual nuclearity, the parent cage (in the most cases a Platonic solid) and the map operation sequence (eventually by its m-factor, see below). When obtained by SW edge-rotation, the suffix RO is added.

Composite operations, like leapfrog *Le*, quadrupling Q and capra *Ca*, and some generalized map operations [51] obey the truncated pyramid volume formula in calculating the nuclearity, in a 3-valent transformed map:

$$m = (a^2 + ab + b^2); \quad a \geq b;\ a + b > 0$$

with m being the multiplication factor ($m = v/v_0$) by a given operation. Thus, *Le* is: (1,1); $m = 3$; Q is: (2,0); $m = 4$ and Ca/S_1 corresponds to (2,1); $m = 7$. The operation sequences, like $Q(Le(G))$, cumulate the m-factor of each of its operations; in the above case $m = 3 \times 4 = 12$. Note that $Q(Le(G)) = Le_{2,2}(G)$, as a single generalized operation.

The most frequently encountered patterns in flower covering are illustrated in Figs. 2–5. Flowers vary in core size c_s (function of the embedding surface) and petale-arrangement, which gives the type of flower. Those with $s = 6$ are considered normal flowers (designable on the graphite sheet) while those of $s > 6 < s$ are taken as

Coronene = [6:6_6]Fw; [6]radialene
v=24; K: $(0,3^6)$

[8]Corannulene = [8:6_8]Fw; [8]radialene
v=32; K: $(0,3^8)$

Fig. 2 Corannulenic flowers

[6]Sumanene = [6:$(5,6)_3$]Fw
v=21; K: $(3(0,3)^3)$

[8]Sumanene = [8:$(5,6)_4$]Fw
v=28; K: $(4(1,2),(1,3))^2$)

Fig. 3 Sumanenes

[6]Corazene = [6:$(5,7)_3$]Fw
v=24; K: $(3(1,3)^3)$

[8]Corazene = [8:$(5,7)_4$]Fw; v=32
K: $(4(2,2)^4)$

Fig. 4 Corazenes

[4]Corazulene-c = [4:$(7(5c))_4$]Fw; [4]radialene
v=28; K: $(0(3,1),(3,2))^2$)

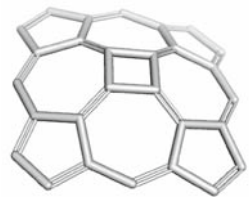

[4]Corazulene-d = [4:$(7(5d))_4$]Fw; [4]radialene
v=32; K: $(0(3(2))^4)$

Fig. 5 Corazulenes

Table 1 Data for hydrocarbon flowers

	Name	Fw	Sym.	HF (PM3)	HOMO-LUMO gap	SE POAV1	HOMA	HOMA core/petal	HOMA contour
	1	2	3	4	5	6	7	8	9
1	[6]Coronene	$[6{:}6_6]$	D_{6h}	2.415	7.227	0	0.739	0.599 0.775	0.715
2	[6]Corazene	$[6{:}(5,7)_3]$	C_{3h}	5.445	6.230	0	0.267	0.714 0.222	0.259
3	[6]Sumanene	$[6{:}(5,6)_3]$	D_{3h}	10.109	2.850	0	0.193	0.809 0.267	−0.350
4	[8]Corannulene	$[8{:}6_6]$	D_{2d}	4.182	6.894	0.411	0.614	0.220 0.718	0.654
5	[8]Corazene	$[8{:}(5,7)_4]$	S_4	6.460	5.381	0.316	0.136	0.629 0.032	0.370
6	[8]Sumanene	$[8{:}(5,6)_4]$	D_{2h}	5.264	5.772	0	0.135	0.004 −0.148	0.466
7	[5]Corannulene	$[5{:}6_5]$	C_{5v}	4.640	7.967	0	0.607	0.841 0.551	0.259
8	[4]Corazulene-c	$[4{:}(7(5c))_4]$	C_{2v}	7.518	5.709	1.035	0.006	−0.430 0.135	0.242
9	[4]Corazulene-d	$[4{:}(7(5d))_4]$	S_4	6.443	6.228	0	0.022	−0.534 0.073	0.272

Heat of formation per atom, HF (kcal/mol); HOMO-LUMO gap (eV); HF/Gap ($\times 100$; eV; PM3); Strain energy per atom, SE (kcal/mol; POAV1) and HOMA index of aromaticity

defects. The planar structures are given in the most important Kekulé valence structure, as drown by our original software JSCHEM [52] at a threshold of 1.415 Å between single and double CC bonds. The π-electron distribution, as given by numeric Kekulé valence structure, are shown in the top of figures (it corresponds to the illustrated valence structure).

Taken as planar hydrocarbons, these patterns show pretty low heat of formation HF and large enough HOMO-LUMO gap for corannulenic flowers (Table 1, entries 1, 4, and 7). Aromaticity in terms of HOMA index is again high for corannulenic flowers but poor for the corazulenic ones, which is also reflected in their higher HF values. [6]Sumanene appears to be the most instable planar structure (Table 1, entry 3), showing anti-aromatic, negative value of HOMA, on contour. However, it is a real molecule, recently synthesized [53,54]. Some strain appear in the non-planar structures (Table 1, entries 4, 5, and 8) [8]Sumanene (Table 1, entry 6) is planar, in contrast to the other [8]annulenes and is far more stable than the normal [6]sumanene.

[5]Corannulene (Table 1, entry 7) shows the highest HOMA value of its core, although it is formally empty in the [5]radialenic Kekulé valence structure. Its contour is, however, much less aromatic. The planar [4]corazulene-d is slightly more stable than the non-planar isomer [4]corazulene-c (Table 1, entries 8 and 9). Their square core is the most anti-aromatic substructure herein discussed.

As a conclusion, aromatic and anti-aromatic substructures coexist and the whole molecules are at most non-aromatic (e.g., [4]corazulenes, Table 1, column 7, entries 8 and 9) up to well defined aromatic structures (e.g., corannulenes, Table 1, column

7, entries 1, 4, and 7). Octagon behaves from non-aromatic ([8]Sumanene, entry 6), through less-aromatic ([8]Corannulene, entry 4) up to aromatic ([8]Corazene, entry 5), depending on the topology of Kekulé valence structure.

3 Design of corazulenic fullerenes

In the following, the various patterns are designed by means of more than one operation sequence. Accordingly, the results will be grouped by patterns and next by operation sequences. The covering is given in term of supra-faces and the multiplication factor m refers to the parent nuclearity. The size of the flowers' core is related to the size of faces of the parent p (Platonic cage), dual d or their double size; to specify the above relatedness the following symbols are used: s_p, s_d, s_{dp} and s_{dd}, respectively. Details of the covering are given in the top of figures.

3.1 Covering by $[n{:}(7(5c))_n]$Fw patterns

The pattern $[n{:}(7(5c))_n]$Fw shows a corazulenic flower in an angular heptagon–pentagon [7(5c)] arrangement. It is provided by the sequences [28,55]: $Tr_s(Q(P_5(G)))$ or $Tr_s(Q(S_2(G)))$. Its SW transform is a sumanenic flower $[2n{:}(5,6)_n]$Fw.

3.1.1 Sequence $Tr_s(Q(P_5(G)))$; $m = 22$

In this sequence, $P_5(O) = P_5(C)$ so that no distinction is possible between the transforms of the dual pair. Figure 6 illustrates two cages covered by the above operation sequence (up to SW transforms). Out of the main flower, the corazulenic $[n{:}(7(5c))_n]$Fw, hexagon-triple [h-triple]co-Fw and hexagons can be evidenced. Table 2 lists the energetic and structural data for the class of cages having $m = 22$. They are open (op), closed (cl) or pseudo-closed (pscl) π-shell cages (Table 2, column 6) and are less strained than C_{60} (column 5). However, the ratio DF/Gap is in favor of C_{60} (with the lowest value—column 4). Also the HOMA index of aromaticity finds the corazu-

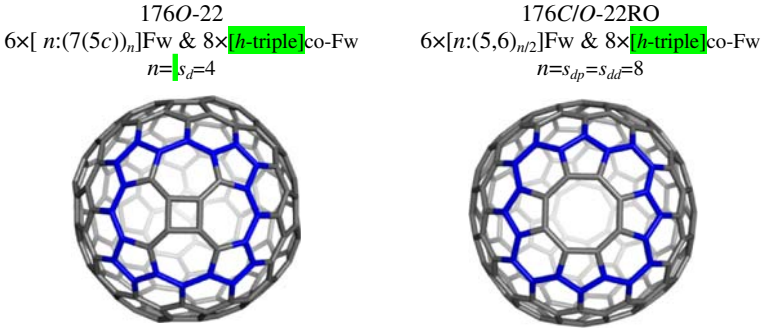

Fig. 6 A corazulenic pattern: $[4{:}(7(5c))_4]$Fw and its SW transform, the sumanenic pattern $[8{:}(5,6)_4]$Fw

Table 2 Data for $Tr_s(Q(P_5(G)))$ corazulenic $[n{:}(7(5c))_n]$Fw cages (of $m = 22$) and their SW isomers

	Cage	Sym.	HF	Gap HF/Gap	SE	E_π shell	HOMA	HOMA-Fw	Fw
	1	2	3	4	5	6	7	8	9
1	88T-22RO	T	11.847	4.051	4.457	1.549	0.316	0.287	$4\times$[6:(5,6)$_3$]
				12.690		op		0.370	$4\times$[h-triple]co-Fw
2	176O-22	O	11.033	3.556	2.865	1.536	0.224	0.111	$6\times$[4:(7(5c))$_4$]
				13.463		cl		0.559	$8\times$[h-triple]co-Fw
3	176C/O-22RO	O	9.436	4.006	2.946	1.549	0.267	0.177	$6\times$[8:(5,6)$_4$]
				10.221		pscl		0.680	$8\times$[h-triple]co-Fw
3	220P_P-22	C_1	11.340	3.263	2.677	1.539	0.165	0.122	$5\times$[4:(7,5)$_c$]
				15.080		Op		−0.137	$2\times$[5:(7,5)$_c$]
								0.677	$10\times$[h-triple]co-Fw
4	220P_P-22RO	C_1	10.395	3.472	2.797	1.547	0.165	0.2504	$5\times$[8:(6,5)$_4$]
				12.991		Op		−0.112	$2\times$[5:(7,5)$_c$]
								0.676	$10\times$[h-triple]co-Fw
4	C_{60}	I_h	13.512	6.593	8.257	1.553	0.944	0.938	$4\times$[5:6$_5$]
				8.893		cl		0.938	$4\times$[6:(5,6)$_3$]co-Fw

Heat of formation per atom, HF (kcal/mol); HOMO-LUMO gap (eV); HF/Gap ($\times$100; eV; PM3); Strain energy per atom, SE (kcal/mol; POAV1); Total π-electron energy, E_π (β-units; simple Hückel) and HOMA index of aromaticity. For comparison, the fullerene C_{60} is included

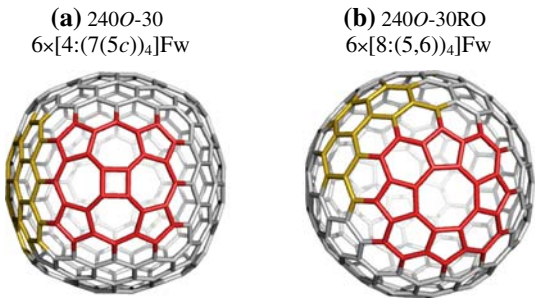

Fig. 7 Corazulenic pattern $[n{:}(7(5c))_n]$Fw, $n = s_d$, changes, by SW, into a sumanenic pattern $[2n{:}(5,6))_n]$Fw

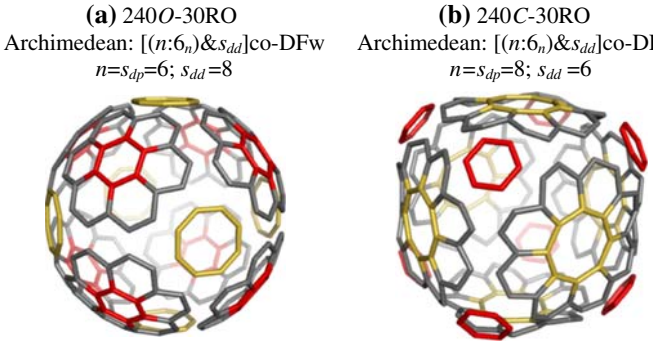

Fig. 8 Difference between the dual-pair rotated transforms of octahedron (**a**) and cube (**b**)

lenic cages less aromatic than C_{60}. The rotated cages, derived from cube/octahedron (Table 2, row 3), appear the most stable in this series.

According to Fowler and Pisanski [14] the π-electronic shells of neutral graphitic cages are classified, function of their eigenvalue spectra, as: (i) *closed*, when $x_{v/2} > 0 \geq \lambda_{v/2+1}$; (ii) *pseudo-closed*, in case $x_{v/2} > x_{v/2+1} > 0$; (iii) *meta-closed* (mcl), with $0 \geq x_{v/2} > x_{v/2+1}$ and (iv) *open*, when the $(v/2)$th (HOMO) and $(v/2+1)$th (LUMO) molecular orbitals are degenerate, $x_{v/2} = x_{v/2+1}$.

Observe in Table 2, the co-Fws remain unchanged, under SW isomerization. The symbol P_p refers to pentagonal prism.

3.1.2 Sequence $Tr_s(Q(S_2(G)))$

The multiplication factor is $m = 10d_0$ (with d_0-the vertex degree), in the triangulated Platonic parent, or $m = 30$ in the trivalent dual [55]. The main pattern, corazulenic $[n{:}(7(5c))_n]$Fw, $n = s_d$ changes by SW into sumanenic pattern $[n{:}(5,6))_{n/2}]$Fw, $n = s_{dd}$ (Fig. 7).

The used sequence of map operations is non-commutative because of S_2. This implies the clear difference between the dual-pair rotated transforms (Fig. 8 and Table 3, rows 3 and 4). This is more evident for the corannulenic co-Fw which, in the 30RO-series, is Archimedean: $[(n{:}6_n)\&s_{dd}]$DFw, $n = s_{dp}$. Observe the co-Fw remains unchanged, under the SW isomerization (Table 3, rows 2 and 3).

Table 3 Data for $Trs(Q(S_2(G)))$ corazulenic $[n{:}(7(5c))_n]$Fw cages (of $m = 30$) and their SW isomers

	Cage	Sym.	HF	Gap HF/Gap	SE	E_π shell	HOMA	HOMA-Fw	Fw
	1	2	3	4	5	6	7	8	9
1	120*T*-30RO	T_h	9.579	5.640	4.792	1.563	0.402	0.365	$4\times[6{:}(5,6))_3]$
				7.370		cl		0.502	$4\times[6{:}6_6]$co-DFw
2	240*O*-30	O_h	9.371	4.783	2.357	1.545	0.205	−0.022	$6\times[4{:}(7(5c))_4]$
				8.502		cl		0.645	$8\times[6{:}6_6]$co-Fw
3	240*O*-30RO	O_h	7.283	5.273	2.107	1.558	0.386	0.290	$6\times[8{:}(5,6)_4]$
				5.993		cl		0.528	$8\times[6{:}6_6]$co-DFw
								0.821	$\&6\times s_{dd}; s_{dd} = 8$
4	240*C*-30RO	O_h	12.960	6.175	4.285	1.561	0.044	0.273	$8\times[6{:}(5,6)_3]$
				9.107		cl		−0.086	$6\times[8{:}6_8]$co-DFw
								0.392	$\&8\times s_{dd}; s_{dd} = 6$
5	240*D*-12	I_h	6.584	5.113	2.506	1.569	0.524	0.504[a]	$12\times[5{:}6_5]$DFw[a]
				5.587		cl		0.510[b]	$8\times[6{:}6_6]$Fw[b]
								0.582[c]	$4\times[6{:}6_6]$Fw[c]

Heat of formation per atom, HF (kcal/mol); HOMO-LUMO gap (eV); HF/Gap ($\times$100; eV; PM3); Strain energy per atom, SE (kcal/mol; POAV1); Total π-electron energy, E_π (β-units; simple Hückel) and HOMA index of aromaticity. For comparison, the corannulenic 240*D*-12 (designed from dodecahedron by Le_{22}) is included
[a] [5]radialenic: $(0,3^5)$; [b] Alternating: $(3(0,3)^3)$; [c] [6]radialenic: $(0,3^6)$

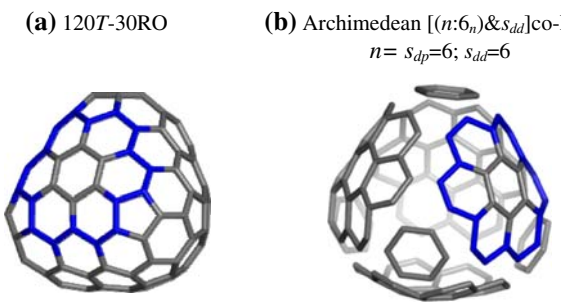

Fig. 9 The most aromatic cage originating in a corazulenic [4:(7(5*c*))$_4$] fullerene; it is derived from tetrahedron by $Tr_S(Q(S_2(G)))$

Remark the highest aromatic character of 120*T*-30RO, (HOMA = 0.402, Table 3, row 1, column 7), in spite of the highest value of strain (4.792 kcal/mol on the whole molecule, distributed as: 6.154:[6:(5,6))$_3$]Fw and 3.7324:[6:6$_6$]Fw. This is due to the coronene [6:6$_6$] contribution but also to the presence of benzene ring in the top flower [6:(5,6))$_3$], in the Archimedean covering (see above and Fig. 9).

Also remark the cage 240*O*-30 (Table 3, row 2): coronene [6:6$_6$]Fw is far more aromatic than the corazulene [4:(7(5*c*))$_4$]Fw (Table 3, row 2, columns 8 and 9).

The most stable structure of this series is 240*O*-30RO (as suggested by the lowest value of HF/Gap, Table 3, row 3, column 4), but all these hypothetical fullerenes (derived from corazulenic cages) show closed π-shell (column 6) and appear as extremely stable. The high stability of this cage comes out from the massive presence of (disjoint) coronene units, which are counted: 8×[6:6$_6$]DFw, but 12×[6:6$_6$]Fw as superposed units [55]. The six octagons in this cage show a large HOMA value, i.e., aromaticity, in contrast to the expected anti-aromatic behavior of this ring (column 8).

Compared to the 240*T*-30 cages, 240*D*-12 (Table 3, row 5) designed from dodecahedron by *Le*&*Q* sequence or by the generalized operation Le_{22}, is even more stable, as its covering is entirely corannulenic, with large HOMA values. According to the main pattern, it shows a Platonic disjoint 12×[5:6$_5$]DFw covering.

An algorithm, developed by Vukičević, [9,56,57] was used to find the Kekulé structure count of corazulenic 240*O*-30 fullerene: $K = 2,423,740,251,144,960$. The corannulenic fullerene 240*D*-12 shows $K = 21,587,074,966,666,816$, which is one order of magnitude larger than for the corazulenic isomer. This supports the conclusion that corannulenic fullerene 240*D*-12 is the most aromatic/stable isomer among the herein investigated 240-isomers; it shows the lowest ratio HF/Gap (5.587) but the highest HOMA value (0.524). Of course, such huge numbers are useless and the researcher must find the far less number of equivalence classes of the geometrical Kekulé structures, as suggested by Randić and coworkers [9].

3.2 Covering by [*n*:(7(5*d*))$_n$]Fw patterns

Several sequences of map operations lead to the corazulenic [*n*:(7(5*d*))$_n$]Fw, $n = s_d$ pattern. Its SW transform is a corazenic flower [2*n*:(5, 7)$_n$]Fw .

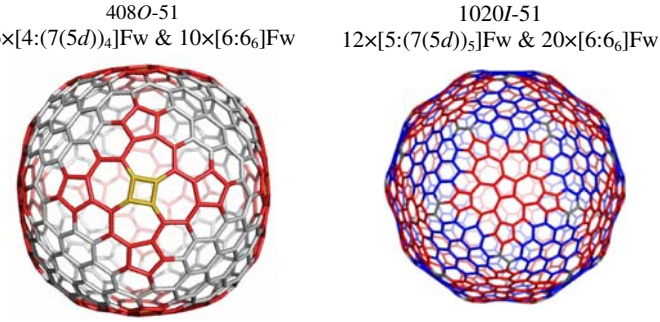

Fig. 10 Covering by $Tr_s(S_1(S_2((G))))$ in two different embeddings

Table 4 Data for $Tr_s(S_1(S_2(G)))$ corazulenic $[n{:}(7(5d))_n]$Fw cages (of $m = 51$) and their SW isomers

	Cage	Sym.	HF	Gap	SE	E_π shell	HOMA	HOMA-Fw	Fw
	1	2	3	4	5	6	7	8	9
1	204*T*-51RO	*T*	11.190	3.808	3.470	1.553	0.234	−0.074	$4\times[6{:}(5,7)_3]$
						pscl		0.313	$4\times[6{:}6_6]$co-Fw[a]
2	408*O*-51	*O*	7.532	3.330	1.466	1.556	0.503	0.340	$6\times[4{:}(7(5d))_4]$
						Cl		0.631	$8\times[6{:}6_6]$co-Fw[a]
3	408*O*-51RO	*O*	9.425	3.841	2.195	1.553	0.297	−0.121	$6\times[8{:}(5,7)_4]$
						pscl		0.562	$8\times[6{:}6_6]$co-Fw[a]

Structural, energetic and aromatic parameters: Symmetry, Sym; Heat of formation per atom, HF (kcal/mol); HOMO-LUMO gap (eV); Strain energy per atom, SE (kcal/mol; POAV1); Total π-electron energy, E_π (β-units; simple Hückel) and HOMA index of aromaticity

[a] There are also naphthalene and pyrene as co-Fws

3.2.1 Sequence $Tr_s(S_1(S_2(G)))$

The above sequence generates a corazulenic flower in the $[7(5d)]$ arrangement [28]. $S_1 = Capra$ induces chirality while truncation (of the selected vertices) provides a face-folding of seven in the final trivalent map. The multiplication factor is $m = 17d_0$ in the triangulated Platonic or $m = 51$ in the trivalent dual pair. Note that $S_1(S_2(G)) \neq S_2(S_1(G))$, in words, the operation sequence is non-commutative.

The tiling given by the above sequence is a mixture of corazulenic $[n{:}(7(5d))_n]$Fw, $n = s_d$ and coronenic $[n{:}6_n]$co-Fw, $n = s_{dp}$ (Fig. 10), separated by naphthalene and pyrene units.

Table 4 lists data on cages of this covering. They are pseudo-closed π-shells, except 408*O*-51 (entry 2), a corazulenic cage which shows a closed π-shells (column 6) and the highest aromaticity (column 7). The high value of HOMA index is due to the coronene flowers $[6{:}6_6]$ but the corazulenic $[4{:}(7(5d))_4]$ flower is more aromatic than in other cages (see the next tables), maybe a consequence of the size effect (?), also supported by the lowest HF value in this series.

In the RO-series, the covering is: $[n{:}(5,7)_{n/2}]$Fw, $n = s_{dd}$; $[n{:}6_n]$co-Fw, $n = s_{dp}$. The octahedron-derivative 408*O*-51RO is far more stable than that of its dual pair 408*C*-51RO, the last one being not included in Table 4.

3.2.2 Sequence $Tr_s(S_{1f}(Q(G)))$

In the sequence of title, Q is the quadrupling map operation, S_{1f} represents the septupling operation performed so that the original faces of M remain untransformed and Tr_s is the truncation of selected vertices. The sequence leads to a Platonic disjoint corazulenic $[n{:}(7(5d))_n]$DFw, $n = s_d$, chiral (by virtue of $S_1 = Ca_{2,1}$) covering; the co-Fw shows a sumanenic $[n{:}(5,6)_{n/2}]$Fw, pattern which forms an Archimedean $[n{:}(5,6)_{n/2}\&s_d]$co-DFw, $n = s_{dp}$ covering (see below).

The sequence $(Q\&S_{1f}\&Tr_s)$ is equivalent to the generalized [51] "DAZU" operation and its multiplication factor is $m = 8d_0$ in the triangulated Platonic or $m = 24$ in the trivalent dual pair. Table 5 lists data for cages of $m = 24$.

Of particular interest [55] is here the SW rotation of the spokes of the n-gonal hub of $[n{:}(7(5d))_n]$Fw. It leads to a Platonic covering by disjoint corazenic/isocoronenic [58] flowers $[n{:}(5,7)_{n/2}]$. The rotation also changes the sumanenic flower to a corazenic one, so that both Fw and co-Fw are of corazenic type and both are disjoint (see below).

As an alternative tessellation, a Platonic anti-aromatic disjoint covering by pentalenes (i.e., abutting pentagons) can be evidenced (see below). The tessellation by disjoint pentalenes represents a generalized [14,55] perfect Clar structure, in the sense the faces composing the 2-factor represent pentalenic contours.

The tetrahedron is self-dual, so that the SW edge-rotation on 96T-24 provides only one rotated cage 96T-24RO (Table 5, row 2). Moreover, identical Fw (coming out from the parent face) and co-Fw (accounting for the vertex degree of the parent, or the parent face of the dual) are obtained (row 2, column 9). The tessellation of 96T-24RO is a Platonic, by disjoint, corazenic $4\times[6{:}(5,7)_3]$DFw patterns while the alternative tessellation is a Platonic, by anti-aromatic, $12\times$DPentalenes. Figure 12 illustrates the cage 96T-24RO, tessellated by disjoint corazenes (Fig. 12a) and anti-aromatic disjoint pentalenes (Fig. 12b).

The covering of 96T-24 is a Platonic disjoint $[n{:}(7(5d))_n]$DFw, $n = s_d = 3$ while the co-Fw forms an Archimedean disjoint $[n{:}(5,6)_{n/2}\&s_d]$co-DFw, $n = s_{dp} = 6$; $s_d = 3$ covering. Figure 11 illustrates the above coverings.

Between the two 96-cages, the RO-isomer appears more aromatic by the Kekulé structure count K criterion (1,149,200 for 96T-24RO vs. 1,095,664 for 96T-24). The same ordering is given by the energetic criterion HF (which is lower for 96T-24RO, this being classified more stable) but the reverse ordering is suggested by the total π-electron energy E_π and total HOMA index (Table 5, rows 1 and 2, columns 6 and 7). Closer to the K-criterion ordering is that given by local HOMA-Fw values which only account for the flowers (the connections between the disjoined supra-faces are not included).

The transforms by $(Q\&S_{1f}\&Tr_s)$ of the dual-pair, octahedron (covered by $[4{:}(7(5d))_4]$Fw) and cube (with $[3{:}(7(5d))_3]$Fw pattern) provide, by further SW edge-rotation, the only 192C/O-24RO cage (Table 5, row 4). Because of the trigonal faces, 192C-24 could not be optimized and consequently is missing in Table 5. Figure 13 illustrates two distinct, disjoint corazenic flowers (the Fw and its co-Fw) in one and the same cage derived from C/O. Tessellation is Platonic for both Fw/co-Fw and also for the anti-aromatic pentalene covering (see Table 5).

Table 5 Data for $Tr_s(S_{1f}(Q(G)))$ corazulenic $[n{:}(7(5d))_n]$Fw cages (of $m = 24$) and their SW isomers

	Cage	Sym.	HF	Gap HF/Gap	SE	E_π	HOMA	HOMA-Fw	Fw
	1	2	3	4	5	6	7	8	9
1	96T-24	T	16.040	4.580	6.338	1.545	0.190	0.054	4×[3:(7(5d))$_3$]DFw
				15.197		mcl		0.091	4×[6:(5,6)$_3$]co-DFw
								0.567	&4×s_d; $s_d = 3$
2	96T-24RO	T	13.869	4.780	5.348	1.527	0.017	0.098	4×[6:(5,7)$_3$]DFw
				12.590		pscl		0.098	4×[6:(5,7)$_3$]co-DFw
								−0.285	12×DPentalene
3	192O-24	O	12.039	4.755	3.194	1.536	0.173	0.041	6×[4:(7(5d))$_4$]DFw
				10.989		cl		0.267	4×[6:(5,6)$_3$]co-Fw
								0.249	4×[6:(5,6)$_3$]co-Fw
								−1.878	&6×s_d; $s_d = 4$
4	192C/O-24RO	O	15.696	3.866	3.256	1.527	0.033	−0.154	6×[8:(5,7)$_4$]DFw
				17.618		pscl		0.292	8×[6:(5,7)$_3$]co-DFw
								−0.883	24×DPentalene

Heat of formation per atom, HF (kcal/mol); HOMO-LUMO gap (eV); HF/Gap (×100; eV; PM3); Strain energy per atom, SE (kcal/mol; POAV1); Total π-electron energy, E_π (β-units; simple Hückel) and HOMA index of aromaticity

(a) 96*T*-24; Platonic 4×[n:(7(5d))$_n$]DFw, n=s_d=3 **(b)** 96*T*-24; Archimedean [n:(5,6)$_{n/2}$&s_d]co-DFw, n=s_{dp}=6; s_d =3

Fig. 11 Corazulenic pattern [n:(7(5d))$_n$]DFw, $n = s_d$ and its co-Fw

(a) 96*T*-24RO; Platonic [6:(5,7)$_3$]DFw **(b)** 96*T*-24RO; Platonic disjoint pentalenes

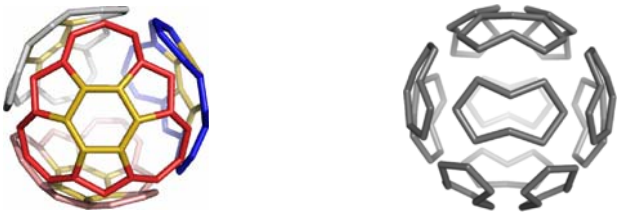

Fig. 12 Aromatic and anti-aromatic patterns: corazene [n:(5, 7)$_{n/2}$]Fw (**a**) and pentalene (**b**)

(a) 192*C*/*O*-24RO; Platonic 6×[8:(5,7)$_4$]DFw **(b)** 192*C*/*O*-24RO; Platonic 8×[6:(5,7)$_3$]co-DFw

Fig. 13 Corazenic disjoint flowers [n:(5, 7)$_{n/2}$]; $n = s_{dp}$ (**a**); $n = s_{dd}$ (**b**)

For corazene/isocoronene [6:(5,7)$_3$], Fowler et al. [58] have recently predicted, in the ipsocentric [37] description, a single, unopposed, intense diatropic perimeter current arising from its four π HOMO electrons; they qualified isocoronene as *super-aromatic*, on the magnetic criterion. By the energetic criterion, the coronene is, however, more stable/aromatic.

As a general trend, the corazulenic flowers are less aromatic than the corresponding co-Fws and the whole molecule is at least non-aromatic, with local manifestation of aromaticity/antiaromaticity (Table 5).

The most stable corazulenic cage of series is 192O-24. It is a Platonic, disjoint corazulenic [4:(7(5d))$_4$]DFw covering, whose pattern is a non-alternant, non-benzenoid one; the co-Fw tessellation is a disjoint Archimedean [n:(5,6)$_{n/2}$&s_d]co-DFw, $n = s_{dp} = 6$; $s_d = 4$. Sumanene [6:(5,6)$_3$]Fw can shows alternating triphenylenic

(a) 120O-15; [n:(7(5c))$_n$ & s_{dp}]JFw; n=s_d=4; s_{dp} =6 Archimedean

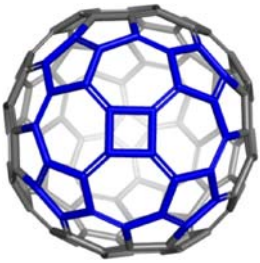

(b) 120O-15; [n:(5,7)$_{n/2}$&s_d]co-JFw; n=s_{dp}=6; s_d =4; Archimedean

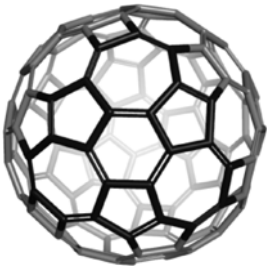

Fig. 14 Two corazulenic flowers tessellating the 120O-15 cage

([6:(0,6)$_3$]Fw)-tripentylenic ([6:(0,5)$_3$]Fw) Kekulé valence structures, as suggested by the HOMA local values (see Table 5, row 3, column 9). The analysis by this geometric criterion also enabled the evidence of other dominant Kekulé valence structures, presented elsewhere [28].

192O-24 shows a generalized perfect Clar structure [28] with the 2-factor designed as corazulenic [4:(7(5d))$_4$] disjoint flowers. With an overall HOMA value of 0.173, the cage 192O-24 is somewhere between non-aromatic and aromatic molecules. In the ipsocentric description, we found [59] for corazulene (the hydrocarbon corresponding to the supra-face [4:(7(5d))$_4$]Fw, as appears in 192O-24) to show the magnetic properties of a circulene, with paired counter-rotating paratropic-hub and diatropic-rim currents. In comparison, the isomeric cornaphthalene shows strong local diatropic circulations in separated parts of the perimeter, being a clear support for the regioselectivity of chemical reactions in such (yet hypothetical) molecules.

3.2.3 $Tr_s(Ca_{(3,2)c}(G))$

In the sequence of title, $Ca_{(3,2)c}$ represents the generalized operation $Ca_{(3,2)}$ with the faces of original map cut-off. It provides joint corazulenic flowers [n:(7(5c))$_n$]JFw, $n = s_d$ which can be red [n:(7(5d))$_n$]Fw as well (Fig. 14a); the co-Fw is the joint corazenic [n:(5,7)$_{n/2}$]JFw (Fig. 14b). The joint is, however, not perfect (as in Capra Ca-transforms) but by means of the co-Fws core, thus being an Archimedean covering.

This is the only operation sequence that put together two corazulenic patterns, being in a mutual relation by SW. The multiplication factor is $m = 5d_0$ in the triangulated Platonic or $m = 15$ in the trivalent dual-pair [55].

Rotating the spokes of the corazulenic flowers of 60T-15 results in 60T-15RO which is just C_{60}(Table 6(8), row 2). The transformed by $Ca_{(3,2)_c}$&Tr_s) of either octahedron ([4:(7(5c))$_4$]Fw) or cube ([3:(7(5c))$_3$]Fw) provide, after SW edge-rotation, one and the same 120C/O-15RO cage (Table 6, row 4). It is covered by sumanenes [n:(5,6)$_{n/2}$], both as Fw and co-Fw, in Archimedean coverings (Fig. 15): [n:(5,6)$_{n/2}$&s_{dp}]JFw; $n = s_{dd} = 8$; $s_{dp} = 6$ and [n:(5,6)$_{n/2}$&s_{dd}]co-JFw, $n = s_{dp} = 6$; $s_{dd} = 8$.

Except 60T-15, which includes triangles, the other members of the series are extremely stable (column 4), closed π-electron shells.

Table 6 Data for $Tr_s(Ca_{(3,2)c}(G))$ corazulenic $[n{:}(7(5c))_n]$Fw cages (of $m = 15$) and their SW isomers

	Cage	Sym.	HF	Gap HF/Gap	SE	E_π shell	HOMA	HOMA-Fw	Fw
	1	2	3	4	5	6	7	8	9
1	60T-15	T	21.350	5.360	9.716	1.525	−0.090	−0.153	$4\times[3{:}(7(5c))_3]$
				17.284		cl		−0.026	$4\times[6{:}(5,7)_3]$co-Fw
2	60T-15RO	I_h	13.512	6.593	8.257	1.553	0.944	0.938	$4\times[6{:}(5,6)_3]$
				8.893		cl		0.938	$4\times[6{:}(5,6)_3]$co-Fw
3	120O-15	O	13.717	5.007	4.057	1.514	−0.073	−0.019	$6\times[4{:}(7(5c))_4]$
				11.888		cl		0.017	$8\times[6{:}(5,7)_3]$co-Fw
4	120C/O-15RO	O	12.454	6.014	4.567	1.543	−0.036	−0.054	$6\times[8{:}(5,6)_4]$
				8.986		cl		0.693	$\&s_{dp} = 6$
								0.116	$8\times[6{:}(5,6)_3]$co-Fw
								−0.688	$\&s_{dd} = 8$

Heat of formation per atom, HF (kcal/mol); HOMO-LUMO gap (eV); HF/Gap ($\times$100; eV; PM3); Strain energy per atom, SE (kcal/mol; POAV1); Total π-electron energy, E_π (β-units; simple Hückel) and HOMA index of aromaticity

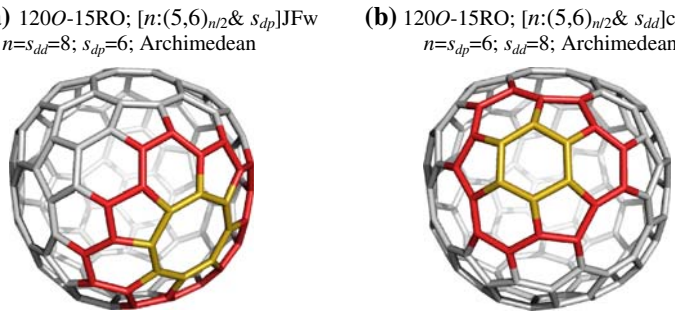

Fig. 15 Two sumanenic patterns $[n{:}(5,6))_{n/2}]$Fw; $n = 8$ (**a**) and $n = 6$ (**b**) in the SW edge-rotated $120O$-15RO cage

The HOMA index does not reflect properly the stability in this series or the aromaticity is not responsible here of the whole stability of a molecule. Note the highest value of this index for C_{60}, which is, however, supra-estimated.

The K-criterion is also in favor of $C_{60} = 60T$-15RO: 12,500 when compared with $60T$-15: 5,096. The same is true for the RO-cage derived from cube/octahedron: $120O$-15RO; 58,083,472 vs. $120O$-15; 46,676,224. In comparison, $120T$-30RO; 136,861,056, expresses the higher stability of this last 120-cage vs. the above isomers [60] (see also Table 3).

3.2.4 Sequence $RO(Tr_{v0}(Ca_{32}(G)))$

This sequence is presented without the implied corazulenic covering, by energetic reasons (cycles R_3 with high strain), so that only the rotated objects are discussed here. The characteristic of this sequence is truncation of the original map vertices Tr_{v0} which provides, when the map is trivalent, a strained flower $[3{:}7_3]$Fw; this gives by SW rotation the corazenic flower $[6{:}(5,7)_3]$Fw. The co-Fw is the corannulenic flower $[n{:}6_n]$Fw; $n = s_p$. The multiplication factor is $m = 7d_0$ in the triangulated Platonic or $m = 21$ in the trivalent dual-pair. Figure 16 illustrated this sequence of operations while Table 7 gives the energetic and topological data for a family of cages. These data show that flowers $[n{:}6_n]$Fw; $n = 5, 6$ support the most of overall aromaticity of these cages, which increases as the size increases and makes the structure more relaxed (see the decreasing trend of the strain—Table 7, column 5) and consequently more stable.

4 Design of benzo-coronenic fullerenes

4.1 Sequence $Tr(St(G))$

Sequence $Tr(St(G))$ provides benzo-coronenic $[n{:}((6)6)_n]$Fw; $n = s_p$ patterns which form Archimedean coverings, with the corannulenic flowers $[4{:}(6)_4]$co-Fw, in case of regular prisms (P_P and P_H stand for pentagonal and hexagonal prism, respectively—Table 8). The multiplication factor is $m = 3d_0$ in the triangulated Platonic or $m = 9$ in

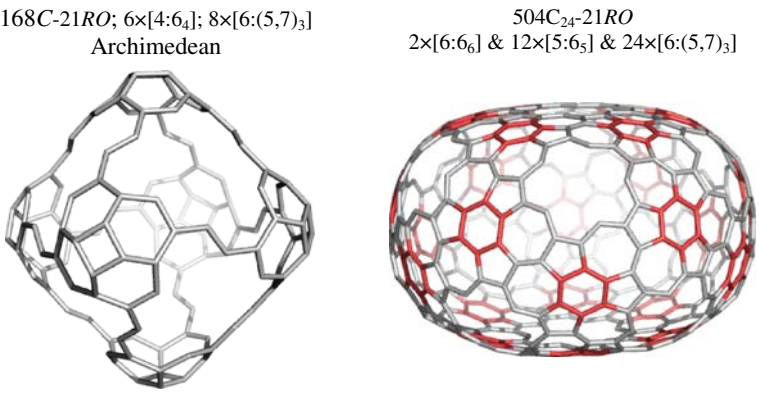

Fig. 16 Cages by the sequence $RO(Tr_{v0}(Ca_{32}(G)))$

Table 7 Data for $RO(Tr_{v0}(Ca_{32}(M)))$ cages

	Cage	Sym.	HF	Gap HF/ Gap	SE	E_π shell	HOMA	HOMA-Fw	Fw
	1	2	3	4	5	6	7	8	9
1	168*C*-21RO	C_1	12.966	5.33	4.52	1.526	0.133	0.388	6×[4:6$_4$]JFw
				10.557		cl		0.042	8×[6:(5,7)$_3$]JFw
2	420*D*-21RO	C_1	8.087	4.870	1.423	1.542	0.328	0.727	12×[5:6$_5$]
				7.206		pscl		0.120	20×[6:(5,7)$_3$]
3	504/C_{24}-21RO	C_2	7.480	4.7	1.324	1.552	0.318	0.7413	12×[5:6$_5$]
				6.904		pscl		0.533	2×[6:6$_6$]
								0.1314	24×[6:(5,7)$_3$]

Heat of formation per atom, HF (kcal/mol); HOMO-LUMO gap (eV); HF/GAP (×100; eV; PM3); Strain energy per atom, SE (kcal/mol; POAV1); Total π-electron energy, E_π (β-units; simple Hückel) and HOMA index of aromaticity

Table 8 Data for $Tr(St(M))$ cages and their SW isomers

	Cage	Sym.	HF	Gap HF/ Gap	SE	E_π shell	HOMA	HOMA-Fw	Fw
	1	2	3	4	5	6	7	8	9
1	72*C*-9	O_h	17.230	6.479	9.250	1.542	0.039	−0.022	2×[4:((6)6)$_4$]JFw
				11.540		cl		0.117	4×[4:6$_4$]JFw
2	90P_P-9	C_{5h}	14.654	6.098	7.567	1.550	0.159	0.260	2×[5:((6)6)$_5$]JFw
				10.427		cl		0.165	5×[4:6$_4$]JFw
3	108P_H-9	C_{6h}	15.528	5.735	7.729	1.552	0.119	0.313	2×[6:((6)6)$_6$]JFw
				11.749		cl		0.198	6×[4:6$_4$]JFw

Heat of formation per atom, HF (kcal/mol); HOMO-LUMO gap (eV); HF/Gap (×100; eV; PM3); Strain energy per atom, SE (kcal/mol; POAV1); Total π-electron energy, E_π (β-units; simple Hückel) and HOMA index of aromaticity

the trivalent dual-pair. It appears that the operation sequence is equivalent to $2 \times Le$, so that closed π-electron shells are expected and corresponding good stability (compare to C_{60}, Table 2).

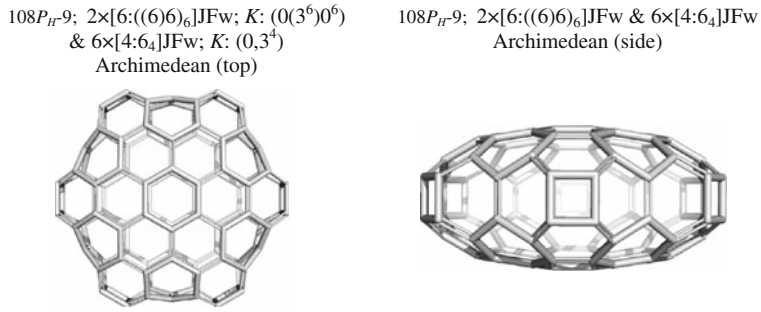

Fig. 17 Benzo-coronenic pattern

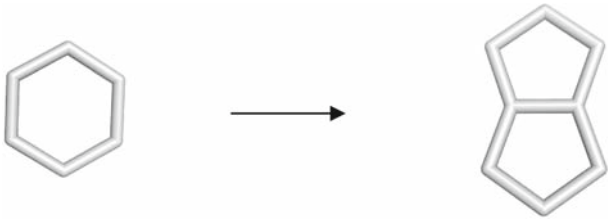

Fig. 18 The Endo–Kroto growth operation

Figure 17 illustrates the object derived from the hexagonal prism; local covering is given in terms of numerical Kekulé π-electron distribution.

5 Retro Endo–Kroto reaction

It is the place to mention another operation, which model the so-called Endo–Kroto [61] reaction (Fig. 18), claimed in the mechanisms of fullerene growth. A C_2 unit is inserted into a hexagonal face, thus increasing the number of carbon atoms of a fullerene. In our case, more interesting is the "retro" operation, denoted *REK*, which leads to the smaller precursor [55].

Several cages having fused pentagons (i.e., pentalenes) can be looked for the *REK* operation: 204*T*-51RO leads to C_{180} (derived from $C_{20} = D$ by *Le*&*Le*) and 300*I*-15 leads to C_{240} (derived from D by $Le_{(2,2)}$). The products of *REK* operations above mentioned are included in the list of the most stable cages herein discussed. Other examples are given in Table 9; the name of these objects includes information on both the original cage and product by *REK*. These objects represent somewhat strained structures, with relatively high HF values. HOMA index classifies them as anti-aromatic or at most non-aromatic (Table 9, columns 7 and 8). They are, however, closed shells, with high HOMO-LUMO gap (column 4). The cage 192*O*_24*RO*_144*REK* (Fig. 19) shows a tessellation equivalent to the "naphthylenic" covering embedded on the torus; its $K = 70, 556, 640, 625$.

Strain energy SE calculations have been performed by JSCHEM software [52] at the POAV1 level of theory [62–65].

Table 9 Data for *Retro Endo–Kroto* cages

	Cage	Sym.	HF	Gap HF/Gap	SE	E_π	HOMA	HOMA-Fw	Fw
	1	2	3	4	5	6	7	8	9
1	96*T*_24*RO*_72*REK*	O_h	17.23	6.479	9.250	1.542	0.039	0.117	6×[4:6_4]
				11.539		cl			
2	192*O*_24*RO*_144*REK*	O_h	20.187	6.937	7.719	1.540	−0.357	0.450	8×[6]
				12.628		cl		−0.229	8×[6:6_6]
								−0.299	6×[8:6_8]
								−0.235	12×[4:6_4]
3	120O_15_96*REK*	O_h	14.152	5.970	7.405	1.550	0.145	0.773	16×[6]
				10.287		cl		0.031	6×[4:6_4]DFw

Heat of formation per atom, HF (kcal/mol); HOMO-LUMO gap (eV); HF/Gap (×100; eV; PM3); Strain energy per atom, SE (kcal/mol; POAV1); Total π-electron energy, E_π (β-units; simple Hückel) and HOMA index of aromaticity

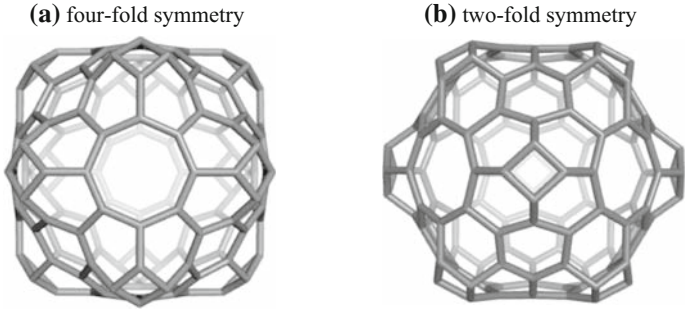

Fig. 19 Tessellation by retro Endo–Kroto operation: $192O\_24RO\_144REK$

6 Conclusions

Sequences of classical or single generalized map operations were used to obtain corannulenic and corazulenic flowers as covering patterns for nanostructures.

The aromaticity of some cages tessellated by these chemically interesting supra-faces is discussed in terms of several criteria. The covering was given as π-electron partition within Kekulé valence structures.

As a structural/geometric parameter of aromaticity, HOMA index enabled evaluation of local aromatic character of the discussed supra-faces and brought evidence for several dominant Kekulé valence structures.

Disjoint corannulenic flower coverings provided fully resonant graphs, associated to the most aromatic/stable structures herein discussed. Next stable cages were those having a disjoint corazulenic ($[n{:}(7(5c))_n]$Fw or $[n{:}(7(5d))_n]$Fw) coverings; these supra-faces were isomerized by the SW edge-rotations. Of particular interest was the SW rotation of $[n{:}(7(5d))_n]$Fw, leading to disjoint corazulenic/isocoronenic flowers $[n{:}(5,7)_{n/2}]$, proved to show *super-aromatic* character, on the magnetic criterion.

New generalized perfect Clar structures, with the 2-factor designed as pentalenes or corazulenic $[4 : (7(5d))_4]$ disjoint flowers have been evidenced. Noticeable in this respect is the "Kekulé-Dewar" valence structure of the cage C_{192}.

Several operation sequences enabled joint flower coverings, with good stability and locally manifested aromatic (or anti-aromatic) character.

A retro Endo–Kroto operation was proposed to go back from cages tessellated with pentalenes (known as anti-aromatic, destabilizing patterns) to the more stable precursors.

All the herein described operations and their products will be helpful in the process of molecular structure elucidation and in guiding researchers in finding novel nano-structured materials.

Acknowledgement The paper is supported by the CEEX 41Romanian Grant, 2006.

References

1. E.C. Kirby, in *From Chemical Topology to Three-Dimensional Geometry*, ed. by A.T. Balaban (Plenum Press, New York, 1997), pp. 263–296

2. M. Bühl, A. Hirsch, Chem. Rev. **101**, 1153–1183 (2001)
3. M. Randić, Chem. Rev. **103**, 3449–3605 (2003)
4. K. Salem, MATCH, Commun. Math. Comput. Chem. **53**, 419–426 (2005)
5. K. Salem, MATCH, Commun. Math. Comput. Chem. **53**, 427–440 (2005)
6. H. Abeledo, G. Atkinson, in *Discrete Mathematical Chemistry*, ed. by P. Hansen, P.W. Fowler, M. Zheng. DIMACS Series, in Discrete Mathematics and Theoretical Computer Science, vol. 51 (American Mathematical Society, Providence, 2000), pp. 1–8
7. S.J. Cyvin, B.N. Cyvin, J. Brunvoll, MATCH, Commun. Math. Comput. Chem. **25**, 105–113 (1990)
8. J.R. Dias, J. Chem. Inf. Model. **45**, 562–571 (2005)
9. D. Vukičević, H.W. Kroto, M. Randić, Croat. Chem. Acta **78**, 223–234 (2005)
10. E. Clar, *Polycyclic Hydrocarbons* (Academic Press, London, 1964)
11. E. Clar, *The Aromatic Sextet* (Wiley, New York, 1972)
12. K. Fries, J. Liebigs Ann. Chem. **454**, 121–324 (1927)
13. W.-Ch. Shiu, P.Ch.B. Lam, H. Zhang, Theochem **4**, 0210 (2000)
14. P.W. Fowler, T. Pisanski, J. Chem. Soc. Faraday Trans. **90**, 2865–2871 (1994)
15. J.R. Dias, J. Chem. Inf. Comput. Sci. **39**, 144–150 (1999)
16. S.J. Cyvin, I. Gutman, *Kekule Structures in Benzenoid Hydrocarbons*. Lecture Notes in Chemistry, vol. 46 (Springer-Verlag, Berlin, 1988)
17. J.R. Dias, Thermochim. Acta **122**, 313–337 (1987)
18. J.R. Dias, J. Chem. Inf. Comput. Sci. **31**, 89–96 (1991)
19. E.C. Kirby, Fullerene Sci. Technol. **2**, 395–404 (1994)
20. E.C. Kirby, MATCH, Commun. Math. Comput. Chem. **33**, 147–156 (1996)
21. E.C. Kirby, in *Nanostructures-Novel Architecture*, ed. by M.V. Diudea (NOVA, New York, 2005), pp. 175–191
22. S. Nikolić, N. Trinajstić, Gazz. Chim. Ital. **120**, 685–689 (1990)
23. I. Gutman, S. Cyvin, MATCH, Commun. Math. Comput. Chem. **30**, 93–102 (1994)
24. I. Gutman, S.J. Cyvin, V. Petrovic, A. Teodorovic, Polycyclic Aromat. Compds. **4**, 183–189 (1994)
25. D.J. Klein, H. Zhu, in *From Chemical Topology to Three-Dimensional Geometry*, ed. by A.T. Balaban (Plenum Press, New York, 1997), pp. 297–341
26. V. Eberhard, *Zur Morphologie der Polyeder* (Teubner, Leipzig, 1891)
27. P.W. Fowler, Chem. Phys. Lett. **131**, 444–450 (1986)
28. M.V. Diudea, Phys. Chem. Chem. Phys. **7**, 3626–3633 (2005)
29. M.V. Diudea, Forma (Tokyo) **19**, 131–163 (2004)
30. M.V. Diudea, in *Nanostructures-Novel Architecture*, ed. by M.V. Diudea (NOVA, New York, 2005), pp. 203–242
31. M.V. Diudea, in *Nanostructures-Novel Architecture*, ed. by M.V. Diudea (NOVA, New York, 2005), pp. 111–126
32. M. Stefu, M.V. Diudea, *CageVersatile 1.3* ("Babes-Bolyai" University, Cluj, 2003)
33. H. Hosoya, Y. Tsukano, K. Nakada, S. Iwata, U. Nagashima, Croat. Chem. Acta **77**, 89–95 (2004)
34. H. Hosoya, Y. Tsukano, M. Ohuchi, K. Nakada, in *Computer Aided Innovation of New Materials II*, ed. by M. Doyama, J. Kihara, M. Tanaka, R. Yamamoto (Elsevier, Amsterdam, 1993), pp. 155–158
35. E. Clar, U. Sanigok, M. Zander, Tetrahedron **24**, 2817–2823 (1968)
36. J.M. Schulman, R.L. Disch, J. Phys. Chem. A **101**, 9176–9179 (1997)
37. T.A. Keith, R.F.W. Bader, Chem. Phys. Lett. **210**, 223–231 (1993)
38. P. Lazzeretti, in *Progress in Nuclear Magnetic Resonance Spectroscopy*, vol. 36, ed. by J.W. Emsley, J. Feeney, L.H. Sutcliffe (Elsevier, Amsterdam, 2000), pp. 1–88
39. A. Acocella, E.W.A. Havenith, E. Steiner, P.W. Fowler, L.W. Jenneskens, Chem. Phys. Lett. **363**, 64–72 (2002)
40. A. Julg, Ph. Francois, Theor. Chim. Acta **7**, 249–261 (1967)
41. A. Julg, in *Aromaticity, Pseudoaromaticity, Anti-Aromaticity*, ed. by E.D. Bergmann, B. Pullman (Israel Acad. Sci. Human., Jerusalem, 1971), p. 383
42. C.W. Bird, Tetrahedron **41**, 1409–1414 (1985)
43. T.M. Krygowski, J. Chem. Inf. Comput. Sci. **33**, 70–78 (1993)
44. T.M. Krygowski, A. Ciesielski, J. Chem. Inf. Comput. Sci. **35**, 203–210 (1995)
45. T.M. Krygowski, A. Ciesielski, J. Chem. Inf. Comput. Sci. **35**, 1001–1003 (1995)
46. M.J.S. Dewar, Angew. Chem. Int. Ed. Engl. **10**, 761–870 (1971)
47. K. Jug, A.M. Koester, J. Phys. Org. Chem. **4**, 163–169 (1991)

48. A.T. Balaban, D.C. Oniciu, A.R. Katritzky, Chem. Rev. **104**, 2777–2812 (2004)
49. P.W. Fowler, D.J. Collins, S.J. Austin, J. Chem. Soc. Perkin Trans. **2**, 275–277 (1993)
50. A.J. Stone, D.J. Wales, Chem. Phys. Lett. **128**, 501–503 (1986)
51. M.V. Diudea, M. Ştefu, P.E. John, A. Graovac, Croat. Chem. Acta **79**, 355–362 (2006)
52. Cs.L. Nagy, M.V. Diudea, *JSCHEM Software* ("Babes-Bolyai" University, Cluj, 2006)
53. H. Sakurai, T. Daiko, T. Hirao, Science **301**, 1878 (2003)
54. H. Sakurai, T. Daiko, H. Sakane, T. Amaya, T. Hirao, J. Am. Chem. Soc. **127**, 11580–11581 (2005)
55. M.V. Diudea, Cs.L. Nagy, *Periodic Nanostructures*, Chap. 6 (Springer, 2007)
56. M.V. Diudea, D. Vukičević, J. Nanosci. Nanotechnol. **7**, 1321–1328 (2006)
57. D. Vukičević, M. Randić, Chem. Phys. Lett. **401**, 446–450 (2005)
58. A. Ciesielski, M.K. Cyranski, T.M. Krygowski, P.W. Fowler, M. Lillington, J. Org. Chem. **71**, 6840–6845 (2006)
59. M. Endo, H.W. Kroto, J. Phys. Chem. **96**, 6941–6944 (1992)
60. M.V. Diudea, Phys. Chem. Chem. Phys. **4**, 4740–4746 (2002)
61. S. Chigher, M.V. Diudea, *Kekule Structure Counter 1.1* ("Babes-Bolyai" University, Cluj, 2006)
62. R.C. Haddon, J. Am. Chem. Soc. **109**, 1676–1685 (1987)
63. R.C. Haddon, J. Am. Chem. Soc. **112**, 3385–3389 (1990)
64. R.C. Haddon, J. Am. Chem. Soc. **119**, 1797–1798 (1997)
65. R.C. Haddon, J. Am. Chem. Soc. **120**, 10494–10496 (1998)